Proceedings of the 21st ICSMGE, Vienna, Austria, 14 – 19 June 2026. Pistrol, Adam & Schweiger (eds.)
Published by: ÖGG, Austrian Society for Geomechanics, Salzburg, Austria, ISBN 978-3-9503898-4-5
https://doi.org/10.53243/ICSMGE2026-847

Simplified calibration of hypoplastic model parameters based on grain size distribution characteristics

Joana Bombe, Christoph Schmüdderich, Merita Tafili, Torsten Wichtmann
Chair of Soil Mechanics, Foundation Engineering and Environmental Geotechnics, Department of Civil and Environmental Engineering, Ruhr-Universität Bochum, Germany, joana.bombe@ruhr-uni-bochum.de

Jan Machaček
Institute of Geotechnics, Department of Civil and Environmental Engineering, Technische Universität Darmstadt, Germany

ABSTRACT: Finite Element analyses are increasingly utilized to evaluate the serviceability and stability of geotechnical structures under complex loading conditions. While advanced constitutive models provide a more accurate representation of the stress–strain behavior of soils, simpler models remain more widely used in practical applications. One major reason is the significant effort required to calibrate the parameters of advanced models, which often demand extensive laboratory testing and specialized expertise. To enhance the practical applicability of hypoplastic models, this study proposes a simplified calibration procedure. The objective is to estimate the parameters α and β of the hypoplastic model for sand based on easily measurable soil properties, such as grain size distribution characteristics (d_{50}, C_u). 22 sand mixtures with linear grain size distribution curves (L-sands) were used, varying in d_{50} and C_u. The hypoplastic parameters were determined using the "numgeo Automatic Calibration Tool", based on existing laboratory data (e.g., from oedometer and triaxial tests). Correlations between α, β and d_{50}, C_u were derived and then validated with available data for natural sands. Validation showed good estimates of α and β using the simplified calibration approach. However, some materials showed notable deviations in the element tests. The method's applicability were further validated through a comparative numerical study using a laterally loaded single pile under monotonic horizontal loading. The simulation results show very good agreement in the horizontal pile head displacements between the model with calibrated parameters and the model with correlated parameters. Despite the variations in the element tests, the simplified method offers a reasonable compromise between accuracy and effort for extensive laboratory testing.

KEYWORDS: Hypoplasticity, Simplified calibration, Correlation, Automatic Calibration.

1 INTRODUCTION

Finite Element (FE) analyses are widely used to study geotechnical structures under various loading conditions, including monotonic and cyclic loading. Advanced constitutive models are beneficial for such analyses, as they capture the nonlinear, stress- and density-dependent behavior of soils under complex boundary and loading conditions. Despite the improved accuracy offered by advanced constitutive models, their use in practice remains limited due to the substantial effort and expertise required for the calibration of their parameters. In contrast, simpler constitutive models such as Mohr-Coulomb or Hardening Soil, which do not account for density dependency, remain widely used, not only because they are easier to calibrate, but also because the information required for their calibration is typically less extensive and often readily available from the geotechnical site investigation report. To promote the practical application of advanced constitutive models, particularly hypoplasticity, a simplified and accessible calibration procedure is required. Such a procedure would enable the use of advanced models in the design of complex geotechnical structures based on Finite Element analyses, without imposing excessive demands on time or expertise. Until now, only a few studies (Herle, 1997, Herle and Gudehus, 1999, Meier, 2009) have attempted to simplify the calibration of hypoplastic models. However, there is a lack of reliable correlations for hypoplastic parameters that apply to soils with a wide range of different grain size distributions.

This study aims to develop a simplified calibration approach for the parameters α and β of the hypoplastic model for sand by von Wolffersdorff (1996). The simplified calibration is based on easily obtainable grain size distribution characteristics, specifically the mean grain size d_{50} and the coefficient of uniformity C_u. To this end, a large experimental database is utilized, comprising oedometric compression tests and drained monotonic triaxial tests on 22 different sands with linear grain size distribution curves covering a wide range of d_{50} and C_u. The methodology consists of the following steps:

1. calibration of hypoplastic parameters α and β for all sands using the "numgeo Automatic Calibration Tool" (numgeo-ACT, Machaček et al., 2022),
2. derivation of empirical correlations between hypoplastic parameters (α, β) and grain size distribution characteristics (d_{50}, C_u) and
3. validation of the proposed correlations using data for natural sands not involved in the steps 1 and 2.

2 TESTED MATERIALS AND TEST RESULTS

The grain size distribution curves of the sands considered for the development of the correlations are shown in Figure 1. They were mixed from a natural fluvially deposited quartz sand from a sand pit near Dorsten, Germany. The grain shape is subangular. Prior to mixing, the granular material has been decomposed into 25 gradations with grain sizes between 0.063 mm and 16 mm. The clean sands and gravels L1 to L8 (Figure 1a) have different mean grain sizes in the range $0.1\text{mm} \leq d_{50} \leq 6\text{ mm}$, but the same uniformity coefficient C_u = 1.5. There are two groups of clean sands having the same mean grain size but different C_u-values between 1.5 and 8: L4 and L10 - L16 with d_{50} = 0.6 mm and L6 and L17 - L23 with d_{50} = 2 mm (Figure 1b). For validation of the deduced correlations, three natural clean sands (Bio-Bio sand from Chile, Senftenberg sand from Germany and UWA sand from Australia) with material parameters summarized in Table 1 were used.

Table 1. Index properties of the considered natural sands.

Material	d_{50} mm	C_u -	φ_c °	e_{min} -	e_{max} -
Bio-Bio sand	0.69	2.3	34.3	0.610	0.948
Senftenberg sand	0.39	2.3	32.3	0.427	0.711
UWA sand	0.18	1.67	32.1	0.521	0.788

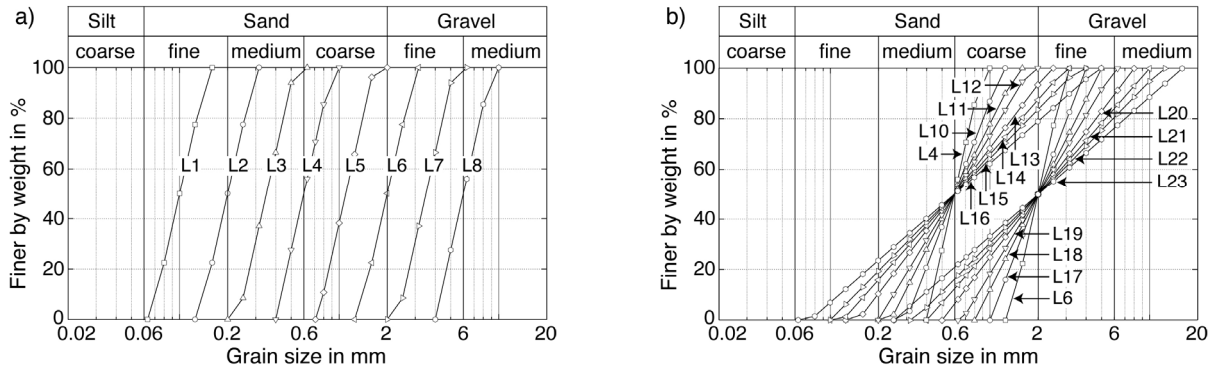

Figure 1. Grain size distribution curves of the 22 sand mixtures (adapted from Wichtmann and Triantafyllidis, 2009).

3 PARAMETER CALIBRATION WITH NUMGEO-ACT

For the calibration of the parameters of the hypoplastic model, the numgeo Automatic Calibration Tool (numgeo-ACT) (Machaček et al, 2022) was used. The numgeo-ACT enables the automatic calibration of advanced constitutive models based on laboratory tests, for instance oedometric and triaxial compression tests. The workflow is shown in Figure 2. First, the laboratory tests are simulated using the FE program numgeo (Machaček, 2020, Staubach, 2022) with an initial estimated set of parameters. The simulation results are then compared with experimental data, and the discrepancy is quantified using a similarity measure (e.g. discrete Fréchet distance). Individual test errors are then combined into a global weighted error, whose change $\Delta\epsilon$ is compared to a predefined tolerance value (TOL). An optimization algorithm iteratively adjusts the parameters until the tolerance is satisfied, or the maximum number of iterations (MAXITER) is reached. In the present study TOL=1e-4 and MAXITER=100 have been used.

The present work employs a two-stage calibration process: First, the critical friction angle φ_c is obtained through cone pluviation tests and the characteristic void ratios e_{c0}, e_{d0}, and e_{i0} are estimated based on tests performed on both the loosest and densest states of the material, while the parameters h_s and n are calibrated using results from an oedometer test on a loose sample (Herle & Gudehus 1999; Herle 1997). Then, the parameters α and β are determined using the ACT, based on drained monotonic triaxial and oedometric compression tests performed with various initial densities. As an example, Figure 3 compares the results of triaxial and oedometer tests (gray) with the corresponding simulations (colored) after calibration.

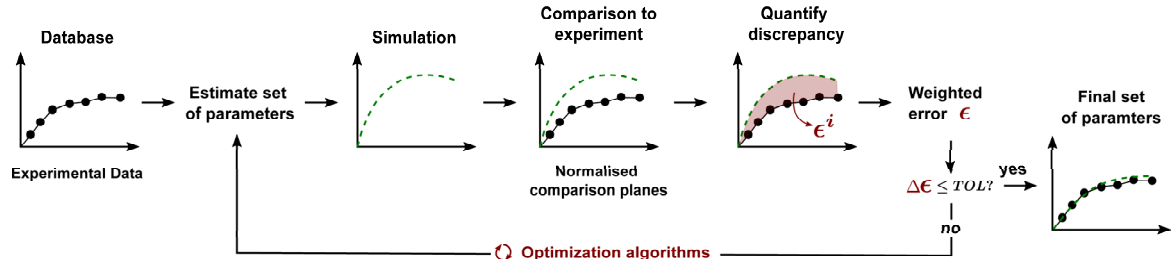

Figure 2. General workflow of numgeo-ACT (Machacek et al. 2025).

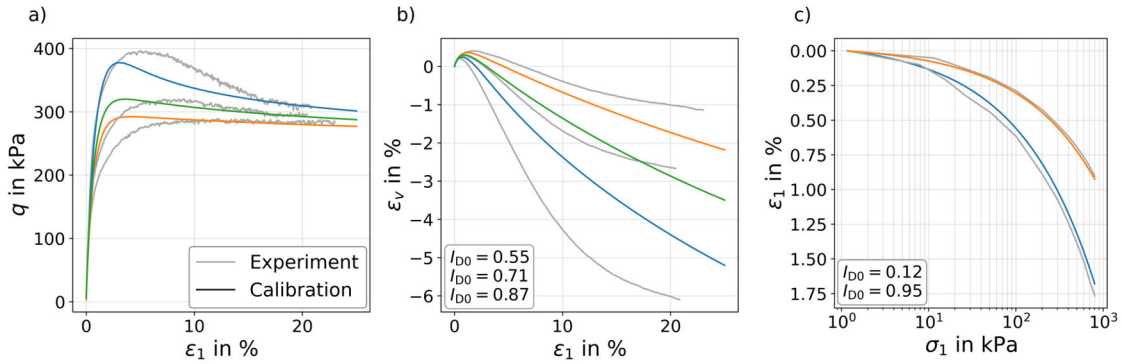

Figure 3. Comparison of experiment and calibration of a), b) drained monotonic triaxial and c) oedometer tests based on L19.

4 SIMPLIFIED CALIBRATION PROCEDURE

As a further simplification to the calibration process, this study examines potential correlations between the parameters α, β and the grain size metrics d_{50} and C_u. They are derived assuming a linear dependency of α and β on d_{50} and C_u and using the calibration results of the L-sands shown in Figure 1 as reference points. If successful, such correlations could reduce the requirement for extensive triaxial and oedometric tests which are rarely available for industry projects. Figure 4 illustrates the procedure: the markers represent the reference L-sands plotted in a C_u vs. d_{50} plane, and the color scale indicates the interpolated α and β values.

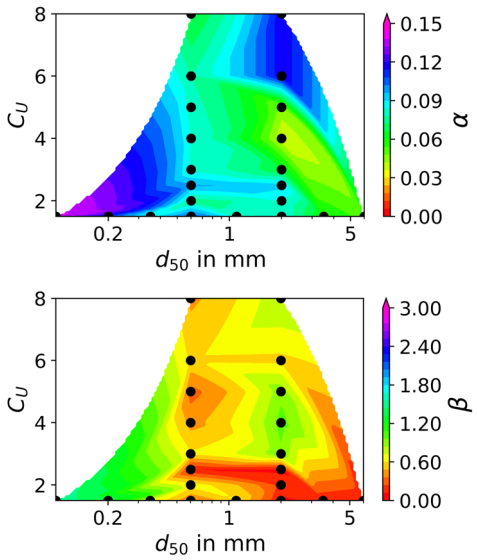

Figure 4. Linear interpolation of α and β.

To validate the simplified calibration approach, data from previously conducted laboratory tests on the natural sands listed in Table 1 were used. As a reference, a full calibration was carried out, following the procedure described in the previous section. The parameters α and β were determined using the numgeo-ACT, while the remaining parameters were manually derived through standard laboratory procedures following Herle & Gudehus (1999) and Herle (1997). In addition, the simplified calibration procedure was applied. In this approach, the correlations were employed to estimate α and β based solely on the grain size distribution metrics d_{50} and C_u, while the other parameters were assigned the values from the reference parameter sets. The essential difference between these two approaches is, therefore, the resulting values of the fitting parameters α and β from each calibration.

Finally, as illustrated in Figure 5 to 7, simulations were performed using both the calibrated parameters and those derived from the correlations. To properly interpret this comparison, it is necessary to understand the distinct roles of these parameters. The parameter α primarily governs the magnitude of the peak deviatoric stress and the development of volumetric strain in triaxial compression tests. In contrast, the parameter β controls the behavior during oedometric compression tests and also influences the initial stiffness in the q-ε_1 plane for triaxial tests.

Note further that a direct comparison between correlation-based numerical and experimental results is not meaningful, since the calibrated simulations already reflect the best average performance attainable with the chosen hypoplastic model across all considered experiments.

Considering the results obtained for Bio-Bio sand depicted in Figure 5, an underestimation of the maximum shear strength as well as dilatancy can be observed for the correlation approach in the triaxial tests on dense samples. Nevertheless, the correlation demonstrates reasonably good agreement with the calibrated curves across all other tests. The curves in the oedometer tests show an almost perfect overlap for both the loose and dense states, even though h_s and n were only calibrated based on the results of the loose sample.

In case of the Senftenberg sand (see Figure 6), the results obtained from calibration and correlation show a better agreement than those of Bio-Bio sand in both the oedometer and triaxial tests. Finally, the results for UWA sand shown in Figure 7 exhibit even closer agreement between calibration and correlation than the other two sands, indicating a particularly good applicability of the simplified approach for this material.

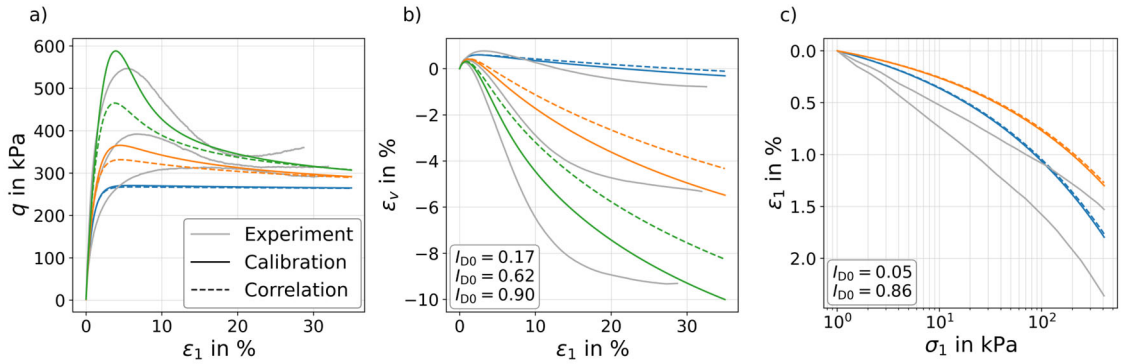

Figure 5. Simulation of a), b) drained monotonic triaxial and c) oedometer tests on Bio-Bio sand (Chile)

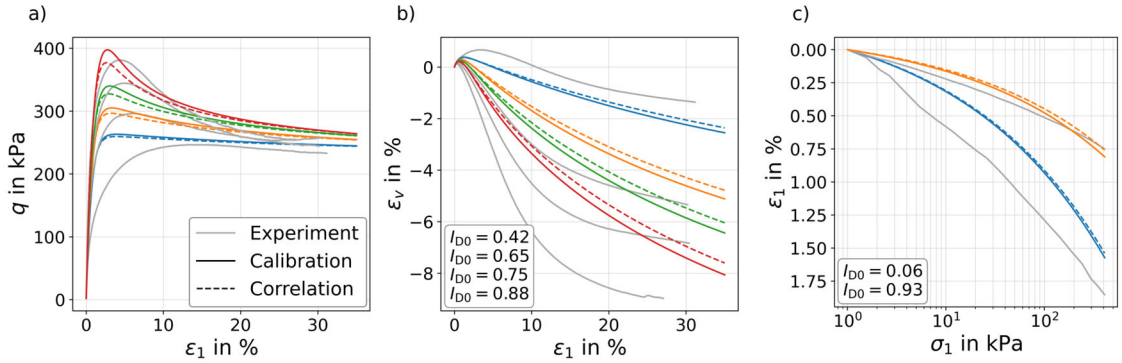

Figure 6. Simulation of a), b) drained monotonic triaxial and c) oedometer tests on Senftenberg sand (Germany)

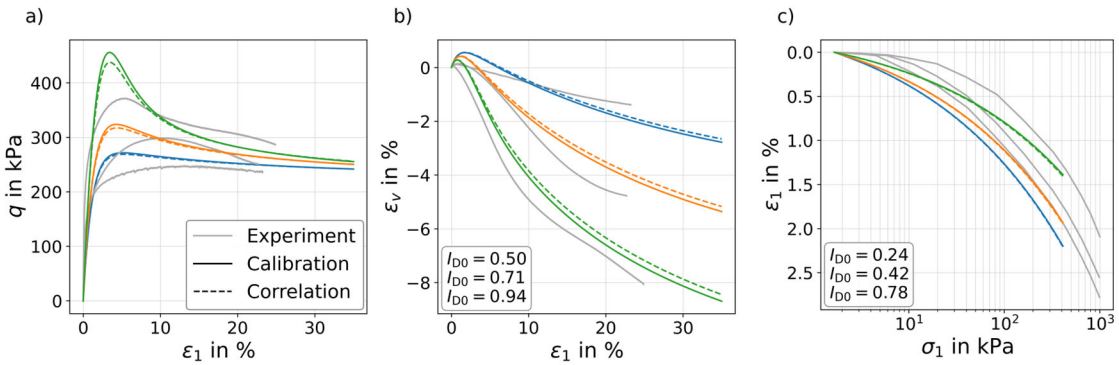

Figure 7. Simulation of a), b) drained monotonic triaxial and c) oedometer tests on UWA sand (Australia).

5 FINITE ELEMENT SIMULATIONS

To further validate the developed correlation approach, a comparative numerical study is conducted using the example of a laterally loaded monopile under monotonic horizontal loading. For this purpose, simulations are carried out using both the calibrated parameter set and the correlated parameter set, applied consistently across three different relative densities of the soil: 25%, 50%, and 75%, representing loose, medium-dense, and dense states, respectively. This setup enables a systematic evaluation of the robustness and practical relevance of the correlated parameters by comparing their performance against the calibrated baseline under identical boundary and loading conditions.

To simulate the lateral behavior of the single pile, a three-dimensional finite element (FE) model was adopted. This model is based on the back-calculation of centrifuge tests of a horizontally loaded single pile embedded in UWA sand, as reported in Machacek et al. (2022b) (Figure 8). Due to the unidirectional nature of the applied load and the symmetry of the boundary value problem, only half of the system was modeled to reduce computational effort without compromising accuracy. The pile is modeled in prototype scale as a hollow steel cylinder with an outer diameter of 1.0 m and an inner diameter of 0.8 m. It extends 4.0 m above the ground surface and is embedded 11.5 m into the soil. A horizontal load of 700 kN is applied at the upper left end of the pile at 4.0 m above the soil surface. The surrounding soil body is represented by a rectangular block with dimensions of 24.5 m in the longitudinal direction (parallel to the load), 12.25 m in the transverse direction, and 17.5 m in height. These dimensions ensure sufficient distance from the pile to minimize boundary effects and capture the stress distribution realistically. The mechanical boundary conditions were chosen in a way that displacements are prohibited in normal direction at the lateral boundaries, including the plane of symmetry. Moreover, vertical and lateral displacements are prohibited at the bottom boundary.

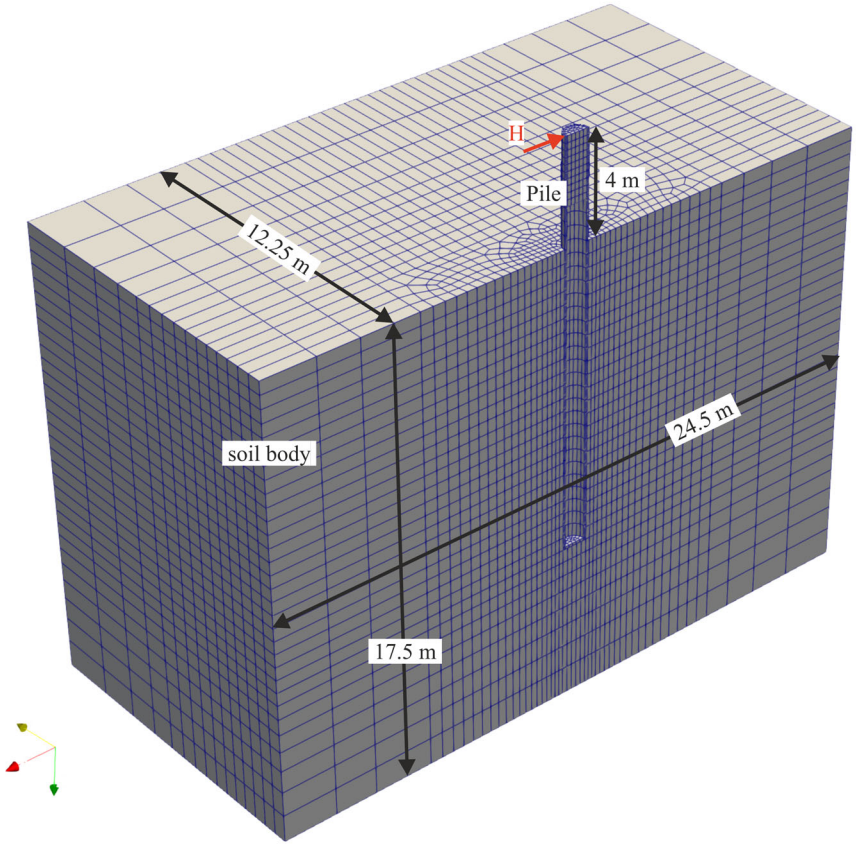

Figure 8. Finite element model of the single pile, adopted from Machacek et al. (2022b).

Mesh refinement is applied in critical regions, particularly in the vicinity of the pile, to ensure accurate resolution of stress gradients and potential nonlinearities. The soil is discretized using reduced integrated, hourglass-stabilized, eight-noded brick elements, which offer computational efficiency and avoid locking effects. The pile itself is modeled using fully integrated eight-noded brick elements. The final finite element mesh consists of 20,573 elements for the soil and 864 elements for the pile. Since dry conditions are assumed throughout the domain, single-phase solid elements are considered for the soil and the pile, discretizing the solid displacements. The interaction between the pile and the surrounding soil is modeled using a mortar contact formulation. Contact constraints are enforced using the penalty method, which allows for small penetrations while maintaining numerical stability. A friction coefficient of 0.2 is applied, corresponding to approx. $1/3\varphi^c$. No separation of contact surfaces is allowed in the normal direction. To avoid zero effective stress at the ground surface and to enhance convergence behavior, a stabilizing compressive pressure of 1 kPa is applied to the top boundary of the soil. The simulation consists of three consecutive calculation steps:

1. In the first step, gravity loading is applied to establish the geostatic stress field. All nodal displacements are constrained during gravity application, and the reaction forces generated at the constrained nodes are recorded for the following step.
2. In the second step, the previously recorded reaction forces are applied as external loads and gradually reduced to zero. During this process, the mechanical boundary conditions are adjusted such that vertical displacements are fixed at the bottom boundary, and horizontal displacements are restrained at the lateral boundaries. The gradual unloading allows the system to transition smoothly from the initial, constrained state to a natural equilibrium. This incremental approach is necessary to account for the nonlinear material behavior of the hypoplastic soil model.
3. Finally, in the third step, a horizontal force of 700 kN is applied incrementally with a linear load ramp over the step time, representing the monotonic increase in lateral loading.

The simulations have been performed using both the calibrated as well as the correlation-based parameters for all three natural tests sands from Section 4. For each sand three relative densities have been investigated: 25 %, 50 %, and 75 %. The results of this study are depicted in Figure 9 in terms of the horizontal pile head displacement over the applied pile head force. Additionally, the relative differences between the two parameter sets for all sands and densities are summarized in Figure 10, showing the deviation between the simulations at maximum load, referenced to the results obtained with the calibrated parameters.

For Bio-Bio Sand, the results shown in Figure 9 demonstrate a very good agreement between the calibrated and correlated parameter sets in the loose and medium-dense states, indicating no significant change in the pile head displacement. In the dense state, a deviation of 0.75 cm at the maximum load is observed, corresponding to 2.7% of total pile head displacement in the calibrated model (Figure 10).

In the case of Senftenberg Sand, small deviations between the predictions obtained using calibrated and correlated parameter sets are apparent across all relative densities. The deviation at maximum load amounts to –0.014 m (–3.7%) in the loose state, –0.015 m (–4.8%) in the medium-dense state, and –0.007 m (–2.7%) in the dense state, each given relative to the pile head displacement calculated using the correlated parameter set. Unlike the trend observed for Bio-Bio Sand, where the deviations increase with increasing density, the largest discrepancy for Senftenberg Sand occurs in the medium dense state. Additionally, the correlation-based results tend to predict slightly larger displacements than the calibrated model.

For UWA Sand, application of the correlated parameters yields larger displacements than the calibrated parameters for the same load level. In the medium-dense state, a deviation of 0.050 m is observed at maximum load, corresponding to 10.0% of total head displacement predicted with the calibrated parameter set. This represents the highest relative deviation among all cases considered. In contrast, the results for the loose and dense states show much higher agreement, with deviations of 2.9% and 1.1%, respectively.

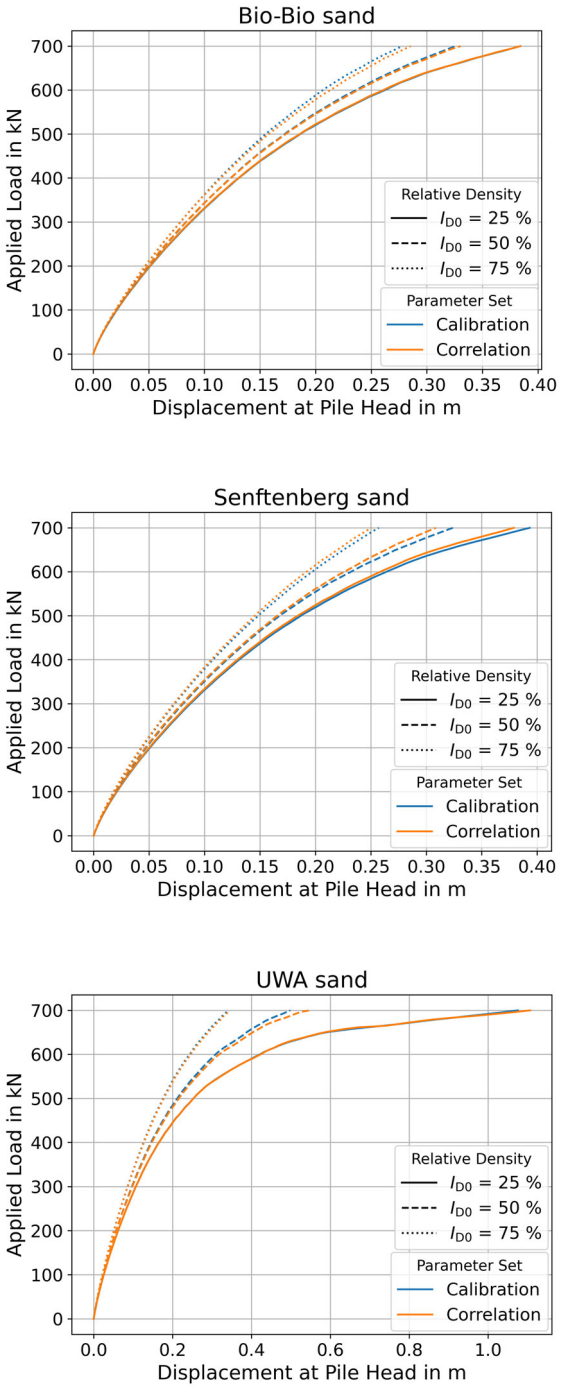

Figure 9. Load-displacement curves at the pile head for Bio-Bio sand (Chile), Senftenberg sand (Germany) and UWA sand (Australia).

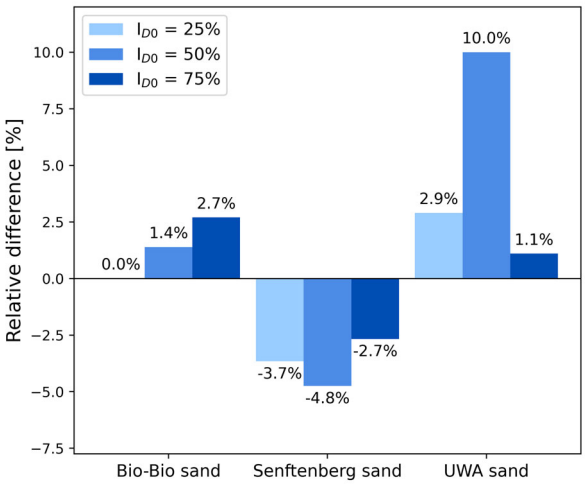

Figure 10. Relative difference in pile head displacement at maximum load relative to the simulation with calibrated parameters.

6 SUMMARY, CONCLUSION AND OUTLOOK

In this study, a simplified calibration approach for the hypoplastic parameters α and β was presented. Considering φ_c, e_{c0}, e_{d0}, e_{i0} estimated from index tests and h_s and n from oedometer tests on loose samples, α and β were calibrated using numgeo-ACT (Machaček et al., 2022) for 22 sands with varying grain size distribution characteristics (d_{50}, C_u). Correlations between α, β and d_{50}, C_u were derived from the calibrated parameter sets and validated based on simulations of laboratory tests on three natural sands. It was shown that overall good estimates of α and β were found using the simplified calibration approach employing the correlations, providing reasonable approximations of the stress-strain behavior observed in lab test simulations. However, for some materials, notable deviations could be detected. Despite these variations, the simplified method offers a good compromise between accuracy and effort required for extensive laboratory testing. The applicability of the approach was further supported by a comparative analysis of horizontal pile head displacements under monotonic lateral loading, which confirmed that the correlated parameters yield sufficiently accurate predictions for practical use. To further decrease the effort associated with the calibration of hypoplastic parameters, it is planned to also consider h_s and n in the simplified calibration, allowing to avoid conducting oedometer tests. Moreover, the effect of grain shape and mineralogical composition may be accounted for in future studies.

7 ACKNOWLEDGEMENTS

The financial support from the German Research Foundation (DFG, project No. 409759834) is gratefully acknowledged.

8 REFERENCES

Herle, I. 1997. Hypoplastizität und Granulometrie einfacher Korngerüste. *PhD thesis. Veröffentlichungen des Instituts für Bodenmechanik und Felsmechanik der Universität Karlsruhe*, Issue No. 142.

Herle, I., and Gudehus, G. 1999. Determination of parameters of a hypoplastic constitutive model from properties of grain assemblies. *Mechanics of Cohesive-frictional Materials: An International Journal on Experiments, Modelling and Computation of Materials and Structures* 4(5), 461-486.

Machaček, J. 2020. Contributions to the Numerical Modelling of Saturated and Unsaturated Soils. *PhD thesis. Veröffentlichungen des Instituts für Bodenmechanik und Felsmechanik am Karlsruher Institut für Technologie (KIT)*, Issue No. 187.

Machaček, J., Staubach, P., Grandas, C., Wichtmann, T., and Zachert, H. 2022. On the automatic parameter calibration of a hypoplastic soil model. *Acta Geotechnica* 17, 5253-5273.

Machaček, J., Brosz, F., Staubach, P., Wichtmann, T. and Zachert, H., 2022. Back-calculations of Centrifuge Tests on Pile Groups Subjected to High-cyclic Loading. DFI-EFFC, *International Conference on Deep Foundations and Ground Improvement: Smart Construction for the Future.* Berlin: Deep Foundations Institute. 534–544.

Machaček, J., Zeng, S. and Taiebat, M., 2025. Enhancing accuracy and efficiency in cyclic liquefaction modeling: An automatic calibration framework for advanced constitutive models. *Computers and Geotechnics*, 183, p.107208.

Meier, T. 2009. Application of hypoplastic and viscohypoplastic constitutive models for geotechnical problems. *PhD thesis. Veröffentlichungen des Instituts für Boden- und Felsmechanik der Universität Karlsruhe*, Issue No. 171.

Staubach, P. 2022. Contributions to the numerical modelling of pile installation processes and high-cyclic loading of soils. *PhD thesis. Veröffentlichungen des Lehrstuhls für Bodenmechanik, Grundbau und Umweltgeotechnik, Ruhr-Universität Bochum*, Issue No. 73.

Von Wolffersdorff, P. A. 1996. A hypoplastic relation for granular materials with a predefined limit state surface. Mechanics of Cohesive-frictional Materials: An International Journal on Experiments, Modelling and Computation of Materials and Structures, 1(3), 251-271.

Wichtmann, T., and Triantafyllidis, Th. 2009. On the influence of the grain size distribution curve of quartz sand on the small strain shear modulus Gmax. *Journal of Geotechnical and Geoenvironmental Engineering, ASCE*, 135(10), 1404-1418.